



Deposited via The University of Sheffield.

White Rose Research Online URL for this paper:

<https://eprints.whiterose.ac.uk/id/eprint/190249/>

Version: Published Version

---

**Article:**

Graves, A., Blanch, O.L., Fernández, D.S. et al. (2022) In-process fingerprints of dissimilar titanium alloy diffusion bonded layers from hole drilling force data. *Metals*, 12 (8). 1353.

<https://doi.org/10.3390/met12081353>

---

**Reuse**

This article is distributed under the terms of the Creative Commons Attribution (CC BY) licence. This licence allows you to distribute, remix, tweak, and build upon the work, even commercially, as long as you credit the authors for the original work. More information and the full terms of the licence here:

<https://creativecommons.org/licenses/>

**Takedown**

If you consider content in White Rose Research Online to be in breach of UK law, please notify us by emailing [eprints@whiterose.ac.uk](mailto:eprints@whiterose.ac.uk) including the URL of the record and the reason for the withdrawal request.

## Article

# In-Process Fingerprints of Dissimilar Titanium Alloy Diffusion Bonded Layers from Hole Drilling Force Data

Alex Graves <sup>1,2</sup>, Oliver Levano Blanch <sup>1</sup> , Daniel Suárez Fernández <sup>1,2</sup> and Martin Jackson <sup>1,\*</sup> 

<sup>1</sup> Department of Materials Science and Engineering, The University of Sheffield, Sir Robert Hadfield Building, Mappin Street, Sheffield S1 3JD, UK

<sup>2</sup> Advanced Manufacturing Research Centre, Advanced Manufacturing Park, Catcliffe, Rotherham S60 5TZ, UK

\* Correspondence: martin.jackson@sheffield.ac.uk

**Abstract:** The manufacture of components that have specific material properties in subcomponent regions is highly desired in many sectors. However, it is challenging to achieve via conventional ingot-wrought and joining processing routes. Recently, diffusion bonding titanium alloy powder using field assisted sintering technology (FAST) has demonstrated that multi-material billets can be manufactured. Such billets still need to be machined into final net shaped components. The machinability and machining strategy of such components needs to be better understood if manufacturing of multi-material components is to be economically viable. This is the first study where drilling machinability of FAST diffusion bonded titanium alloys has been investigated. Location indexed force and torque feedback in-process fingerprinting is utilised during the drilling of multi-material titanium alloy billets. The in-process fingerprinting enabled rapid identification of the types and layering order of alloys within the FAST billets. In addition to force feedback, the hardness, hole surface topography and subsurface microstructure were characterised. Although hardness was found to contribute to variation in bond to bond machinability, results highlighted how alloy chemistry and bond composition are intrinsic to the machining directionality and significantly influence the machined surface quality and process stability. The work demonstrates that machining strategy of multi-material drilling needs to be tailored with respect to direction and diffusion bonded alloy pairing to avoid undesirable surface and subsurface damage at bond locations.

**Keywords:** drilling; field assisted sintering; diffusion bonded; force feedback; hole quality; microstructural damage



**Citation:** Graves, A.; Blanch, O.L.; Fernández, D.S.; Jackson, M. In-Process Fingerprints of Dissimilar Titanium Alloy Diffusion Bonded Layers from Hole Drilling Force Data. *Metals* **2022**, *12*, 1353. <https://doi.org/10.3390/met12081353>

Academic Editors: Shoujin Sun and Massimo Pellizzari

Received: 8 July 2022

Accepted: 4 August 2022

Published: 15 August 2022

**Publisher's Note:** MDPI stays neutral with regard to jurisdictional claims in published maps and institutional affiliations.



**Copyright:** © 2022 by the authors. Licensee MDPI, Basel, Switzerland. This article is an open access article distributed under the terms and conditions of the Creative Commons Attribution (CC BY) license (<https://creativecommons.org/licenses/by/4.0/>).

## 1. Introduction

The implementation of titanium alloys for aircraft components such as engine disks and fan blades has enabled huge weight savings and improved fuel efficiency in the aerospace manufacturing sector. Currently titanium components are machined from near-net shape forgings or bar stock [1]. This is the most proven way to achieve the necessary strength and fatigue performance required to reliably withstand the range of thermal and mechanical stresses put on safety-critical components during flight [2]. However, manufacturing components from forgings or bar stock is not ideal as it can result in regions required to accommodate high stresses being compromised and less demanding regions being over engineered. Due to the non-symmetrical strain path during the open-die forging and heat treatment operations, titanium alloy components exhibit variable micro-textures and anisotropic properties at different billet locations [3].

The allotropic nature of titanium alloys provides a means for manipulating alloy properties through chemical and thermo-mechanical processing [4]. Generally, the majority of titanium alloys used for aircraft are  $\alpha + \beta$  type alloys—Ti-6Al-4V being the most common. Unfortunately, the number of components for which  $\alpha + \beta$  alloys are suitable is becoming saturated. To continue to reduce weight and to improved the performance of critical

components, such as landing gear forgings, aerospace manufacturers have started to use more near- $\beta$  titanium alloys, such as Ti-5553, which have superior strengths and fracture toughness properties [5]. There are only a limited number of applications suitable for titanium alloys regardless of whether an alloy is  $\alpha$ ,  $\alpha + \beta$  or near- $\beta/\beta$ , however, in the future such components could be improved significantly if they can be manufactured using multiple alloys allowing for tailored creep and fatigue resistance at specific locations. The bonding of dissimilar titanium alloys is being considered as a method for the aerospace sector to simultaneously improve component quality, reduce the need for over-engineering and increase the number of applications for which titanium alloys can be utilised [6].

Both linear friction welding (LFW) and friction stir welding (FSW) can be used to create multi-materials from pre-forged material. Considering multi-material components for some applications can provide a design advantage, considering that different locations of the part or component can have site specific properties. However, in LFW and FSW processes, heat affected zones (HAZs) and thermomechanically affected zones (TMAZs) can make it difficult to control the properties and characteristics at the bond region. Hot isostatic press (HIP) technology presents the possibility to join multiple materials or alloys from powder. There are several limitations associated with using HIP to join multiple alloys, including the need to encapsulate the powder in a steel can and slow processing cycles. Such limitations do not apply when using field assisted sintering technology (FAST) to join multiple materials or alloys. Compared to HIP, FAST is a cost effective processing method that is capable of titanium powder consolidation and diffusion bonding of powders into workable billet material. FAST is proven to be more efficient than HIP due to the use of reusable graphite tooling and the process cycle times are 3–4 times faster due to rapid joule heating [7]. FAST also presents a superior option when diffusion bonding multiple materials as it provides flexibility when engineering the exact bond location. The high degree of control during the process means microstructures can be tailored to be optimum for the intended application without any HAZs.

A critical consideration when utilising titanium alloys for aerospace applications is the high costs associated with machining parts to final shape, whilst maintaining the integrity of the part. There are two main reasons for this; (1) often up to 90% of the original forged billet must be removed via the machining process which can require many tools to achieve [8]. (2) The impressive structural properties exhibited by titanium coupled with a low thermal conductivity cause extremely poor machinability and rapid tool wear. This is further exacerbated in the case of near- $\beta$  alloys which are more prone to diffusion bonding with the tool [9–11]. When components are manufactured from a single material from either forged or bar stock, they are naturally over engineered which requires excessive machining to the standard required by the location within the component that is subjected to the highest service stresses. Such stresses typically only occur at specific locations within each part. Extra challenges arise from further post-processing multi-material parts such as chemical compatibility and chip formation mechanisms which if not considered carefully could hinder the service performance. Multi-material components could provide an exceptional opportunity to tailor the mechanical properties of specific locations to accommodate localised stresses thereby providing higher quality components and reducing manufacturing challenges at the machining stage. Currently research into multi-material Ti/CFRP stack drilling has highlighted sequential drilling of dissimilar materials can impact stability and hole quality [12]. There has not been any research into the drilling of diffusion bonded multi-alloy workpieces and so it is not established if there are any similarities to stack drilling. That being said, there has been some research into the machinability of multi-materials; the machining of multi-material aluminum pistons has been investigated by analysing the cutting forces during machining of the parts; showing that there are the fluctuation in force caused by machining several materials in one pass accelerates tool wear [13–16]. Recently, Levano et al., investigated the face-turning machinability of diffusion bonded multiple titanium alloy workpieces (referred to as FAST-DB). Several key phenomena occur when turning FAST-DB titanium alloys,

that could severely reduce machinability including directionality effects, process effects, built-up edge (BUE) and adhered material on the machined surface (pick-up) [17]. In terms of directionality, it was found that the direction in which any two alloys were machined has a direct impact on the damage observed on the machined surface. There was less damage observed when machining from an  $\alpha + \beta$  to  $\beta$  alloy than when the  $\beta$  alloy was machined before an  $\alpha + \beta$  alloys. Since this finding was congruent for all alloys tested researchers concluded the most probable cause the directionality effect on damage was due to the chemical compatibility of alloys. This was supported by the fact that when alloys with similar chemistry's were machined no directionality effects were measured or observed. In the work it was also found that bonds containing certain alloys can be expected to have certain characteristics. For example, bonds containing Ti-5553 showed correlation between force response and surface topography. In general, the work highlighted how multimaterial FAST consolidated billets can face turned effectively, and highlighted aspects of the machinability that should be focused on if the process is to be optimised. In the work by Levano et al., researchers used a force feedback methodology as established by Suarez et al. [18] to investigate machinability. The application of multi-materials within the aerospace industry will require that the methods for investigating and understanding multi-materials machinability are developed for all key machining processes, including drilling. Method development will enable the effect of directionality and alloy chemistry on machinability to be better understood, thereby facilitating cost effective machining strategies that do not compromise the integrity of components to be established. If a force feedback approach is to be utilised in the case of drilling, the interaction of the tool cutting edges with the workpiece and how this impacts torque and thrust force on the spindle must be considered. Unlike turning where there is a relatively small contact point between the tool and workpiece, the whole drill cutting edge influences both force and torque. Analytical modelling of the cutting edge shows that the thrust force is mainly influenced by the action of the chisel, while torque is proportional to the radius, and therefore, is mostly influenced by the cutting edge at the outer corners of the drill tool [19].

If FAST-DB titanium alloys are to be used within the aerospace manufacturing sector, it is crucial that their machinability characteristics for the drilling process are investigated and compared to those previously investigated through turning operations. This will provide tooling manufacturers and machinists the knowledge they require to improve their tools and approaches for machining such multi-materials and functionally graded alloys, in a cost effective manner by improving tool design and optimising process parameters.

This study provides an initial machinability assessment for drilling FAST-DB alloys. This research is required to establish the critical aspects of machinability characteristics in diffusion bonded multi-material drilling. In order to understand the bond characteristics the authors have developed the approach of converting machining force data to reconstruct the individual fingerprint of holes which have been drilled in the FAST-DB titanium workpieces. Fingerprint and diagrams have been reconstructed from signals gathered during single point cutting operation. As a result, this study presents, for the first time, the fingerprint reconstruction during multi-material drilling operations which was used to identify the individual alloy composition and thickness of each layer and which were subsequently correlated to subsurface damage and surface topography.

## 2. Materials and Methods

### 2.1. FAST Sample Manufacture

All billet material used in this investigation was produced from powder. The titanium alloys that have been used are listed in Table 1, which also includes their corresponding nominal elemental compositions (wt.%). These alloys were selected as they are well established and have varying contributions of  $\alpha$  and  $\beta$  stabilising additions. In the study, various combinations of these alloys were diffusion bonded during the solid state FAST process. The alloys were processed into small billets of 60 mm diameter and 14 mm height. Powder stock for each titanium alloy was combined, in layers within a graphite mould

that was then inserted into a field-assisted sintering (FAST) machine. All the samples were processed at 1020 °C for 20 min at a pressure of 28 MPa with a heating rate of 50 °C/min. Once the dwell time finished, the power of the machine stopped and the samples were let to cool down inside the FAST chamber. In total, five FAST-DB multi-material billets were produced, the bonds generated in each plate are listed in Table 2. The order and type of alloys included in each stack were selected to provide a range of different bonds, at different points within each billet. The alloys used in two of the plates were not disclosed to the investigators by the technician who conducted the FAST processing. This constituted a “blind” test, in order to demonstrate the effectiveness of force feedback analysis techniques for characterising the content of the titanium workpieces.

**Table 1.** Titanium alloys and their corresponding nominal compositions (wt.%).

Alloy Name	Nominal Composition (wt.%)
Ti-CP	bal. Ti
Ti-3-2.5	3Al, 2.5V, bal. Ti
Ti-64	6Al, 4V, bal. Ti
Ti-6242	6Al, 4Zr 2Mo 2Sn bal Ti
Ti-5553	5 Al, 5V, 5Mo, 3Cr, bal. Ti
Ti Beta C	3Al, 8V, 6Cr, 4Mo, 4Zr, bal. Ti

**Table 2.** Compositions of the multi-material billets and whether or not the composition of the machined billet was unknown to those analysing the force fingerprint (blind test).

Plate No.	Order of Titanium Alloys in Multi-Material Billets	Blind (Y/N)
1	Ti-64, Beta C	N
2	Beta C, Ti-64, Ti-CP	N
3	Ti-CP, Ti-6242, Ti-64, Ti-5553, BetaC	N
4	Ti-64, Ti-CP, Beta C	Y
5	Ti-3-2.5, Ti-6242, Ti-CP, Ti-5553, Beta C, Ti-64	Y

## 2.2. Machine and Tooling

Machining was conducted on a DMUmonoBLOCK machining centre (DMG Mori., Bielefeld, Germany). Figure 1a shows how billet material was clamped within the machining centre. Torque and x, y, z force was measured using a type Kistler 123C(1111) dynamometer (Kistler, Winterthur, Switzerland) which is shown in Figure 1c and a type 5238B signal conditioner (Kistler, Winterthur, Switzerland). The sampling frequency was 5 kHz, the sensor measuring range for force and torque were 20 kN and 200 Nm, respectively. The tools used are shown in Figure 1b and were 6.9 mm diameter R846, coated TiAlN, solid carbide twist drills and were held within a hydraulic chuck. After every two holes, a new tool was used to minimise the effect of tool wear on the results. In total, four holes were drilled in each plate, the drill was 1845 RPM, the feed was 0.131 mm/rev (industry recommended cutting data for drilling Ti-64). The final two holes were drilled in the opposite direction in each plate, in order to investigate the effect of directionality on the drilling operation.

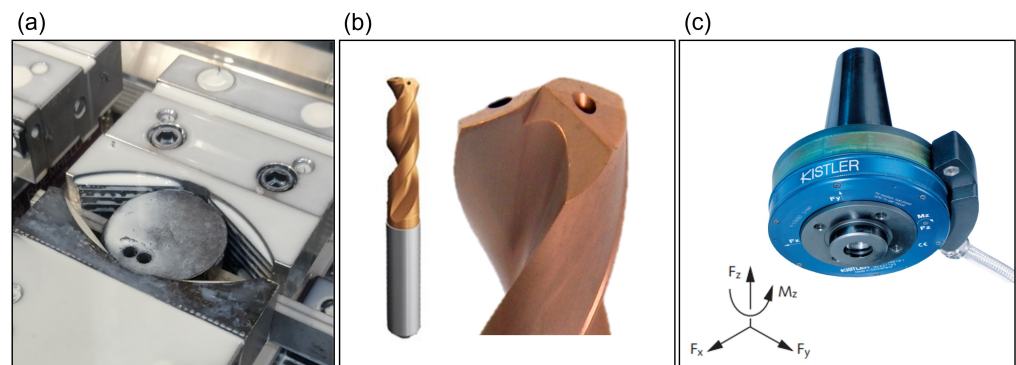


**Figure 1.** (a) Clamped Titanium FAST-DB Billet, (b) Coated Corodrill R846 Tool, (c) Kistler Dynamometer Diagram.

### 2.3. Measurement and Analysis

Each hole was sectioned in half using Struers SiC (10S20) (Struers., Ballerup, Denmark) blades on a Secotom-50 precision cutting machine. Half of each hole was then metallographically prepared and imaged using an Alicona infinifocusSL (Alicona., Berchtesgaden, Germany) optical 3D measurement system, providing a high resolution image and depth point cloud for each hole surface. The second half of each hole was mounted in conductive Bakelite and ground on a Struers Tegramin automatic grinding machine (Struers., Ballerup, Denmark) using 400 then 800, 1200 and 2000 grit papers. Then, samples were polished using a 1 to 10 part  $H_2O_2$  colloidal silica solution before being washed for a further 10 min. An FEI Inspect F50 scanning electron microscope (SEM) was used to image the polished cross sections of holes at the each titanium alloy bond pairing. Vickers hardness measurements of the diffusion bonded billet materials were acquired for the alloy bulk and alloy bond pairings using a DuraScan 80 G5 with a load weight of 1 Kg (HV1). MATLAB programming software (MathWorks, Natick, MA, USA) was used to conduct force feedback analysis from the Kistler data. This involved plotting the spindle torque, x, y, and z forces with location by assigning each data point a position based on the Kistler Dynamometer tachometer signal. MATLAB was then used to plot colour maps of the depth point cloud, spindle torque, x, y and z forces for comparison.

### 2.4. Force Feedback Fingerprint Reconstruction

The force feedback characterisation is a newly developed technique that uses the machining forces captured by a dynamometer to generate 4D diagrams fingerprints where the local machining response of the material is analysed. These diagrams are constructed through the spatial synchronisation of the measured forces/torque based on the drilling parameters where the parameterised 3D tool path is synchronised in time with the dynamometer signal and colour coded based on the machining forces measured at any given point.

This technique has been successfully used for microstructural reconstruction and grain size measurements during turning operations of  $\beta$  titanium alloys by Suárez Fernández et al. [18] and to detect variations in microstructure derived from different heat treatments in Ti-6246 [20]. Moreover, this fingerprint reconstruction provides important insight on dynamic effects that occur during the drilling operation such as chip formation instabilities, chip jamming, or machining vibrations.

The spatial resolution of this technique is dependant on the drilling parameters. This is due to the fact that the sensor acquisition rate is fixed in the time domain (points per second), which defines the speed at which the tool cutting edges travel over the titanium workpiece.

In this study, it is the first time that this type of analysis has been performed in titanium multi-material drilling operations. A Kistler 9123C(1111) drilling dynamometer (Kistler., Winterthur, Switzerland) equipped with a 5221B1 stator was used. In order to capture and digitally store the gathered signals, a Kistler 5070a multi-channel charge amplifier

and data acquisition system were connected to the dynamometer and computer via a USB, respectively. An acquisition rate of 5 kHz combined with a rotational speed of 1845 RPM and a feed per revolution of 0.131 mm. This means that the Z axis resolution is set approximately to 1241 pts/mm and a resolution of 7.5 pts/mm of edge travelled distance, considering a helical path. It is important to note that since the drill has two cutting edges that intersect the central axis, the force response cannot be considered a point to point mapping of the hole, something that can be achieved for surfaces produced in turning [17]. Despite this, the resolution is acceptable for identifying bond locations and is still possible to use the force feedback to compare the machinability and process stability of the drilling operation.

### 3. Results

Table 3 gives the Vickers hardness (HV1) for each alloy. Figure 2 shows the Vickers hardness (HV1) results for alloy bond pairings. The hardness measured for the bond between (the beta alloy) Beta C and (the alpha alloy) Ti-CP has a large range from 300–175 HV and the hardness was seen to decrease across the bond. The hardness variation between Ti-CP and Ti-64 was 215 HV ( $\pm 5$ ). The Ti-64 and Ti-6242 bond and the Ti-5553 to Beta C bond both had a lower hardness value than the respective bulk alloy material, with hardness values of 325 ( $\pm 10$ ) and 290 ( $\pm 8$ ) HV, respectively. In contrast, the bond between Ti-64 and Ti-5553 was much higher than in either alloy at 405 ( $\pm 1$ ) HV. The bond between Ti-64 and Beta C was also higher than the hardness in either alloy but only slightly at 355 ( $\pm 5$ ) HV. Although the hardness of Ti-3-2.5 is not included in Figure 2, it can be expected to behave in a similar manner to Ti-64. Therefore, the bond between Ti-3-2.5 and Ti-5553 will be harder than either Ti-5553 or Ti-3-2.5; as is the case for Ti-5553 and Ti-64.

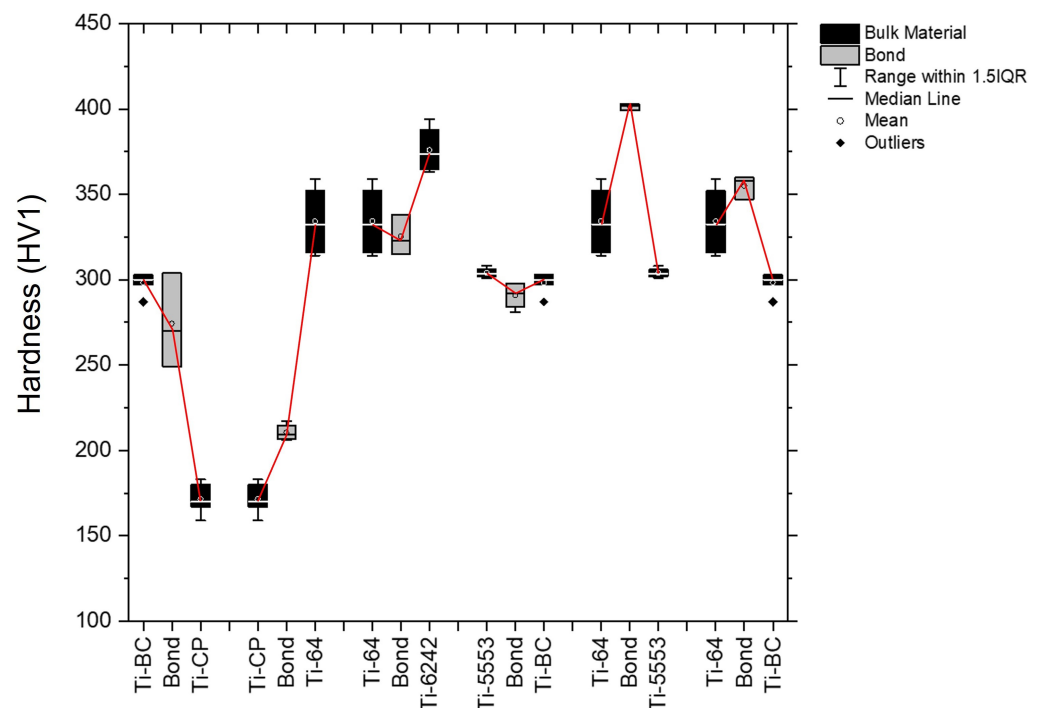


**Figure 2.** Bulk and bond Vickers hardness for alloy pairs where the Vickers hardness indentation load was 1 Kg (HV1).

**Table 3.** Titanium alloys and their corresponding Vickers hardness (indentation load 1 Kg, HV1).

Alloy Name	Vickers Hardness (HV1)
Ti-CP	175 ( $\pm 10$ )
Ti-3-2.5	278 ( $\pm 17$ )
Ti-64	330 ( $\pm 20$ )
Ti-6242	375 ( $\pm 15$ )
Ti-5553	305 ( $\pm 3$ )
Beta C	300 ( $\pm 3$ )

The first FAST-DB billet to be drilled was the sample with two alloys—Ti-64 and Beta C. In Figure 3 comprehensive information around the FAST-DB drilled hole is provided, including a photograph of the surface, surface profile maps and microstructure with respect to the torque (Nm),  $F_y$  (N),  $F_x$  (N),  $F_z$  (N) at the corresponding positions. In the photograph and depth map, adhered material is evidenced and which is in no way related to the bond location. The photograph and depth map also show significant scratches on the machined surface within the Ti-64. The difference between the surface finish of both alloys is clear. The force and torque were both higher in Beta C, the alloy at the bottom half of the billet (Figure 3). Once the drill had penetrated the bond, the required torque to maintain the same rotational speed increased by approximately 20% for a depth of 3–4 mm. During this period of increased torque,  $F_y$  increased by approximately 100 N. In  $F_x$  during and after the bond there was very little change.  $F_z$  decreased slightly, just before the bond was drilled, then proceeded to increase for the next 3–4 mm (as torque increased), before reaching a steady state within the bulk Beta C. The bond is shown clearly in the micrographs in Figure 3. There is a very slight depression in the machined surface before the bond but in general the region remains undamaged for this sample.

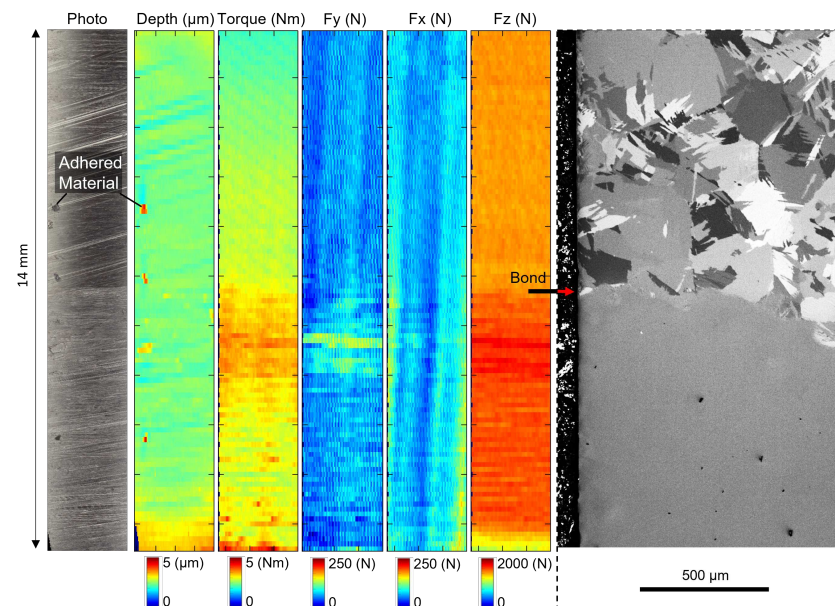


**Figure 3.** A photograph of the drilled surface, micrographs of the bond interfaces and depth, torque,  $F_y$ ,  $F_x$  and  $F_z$  maps for holes drilled at 1845 RPM and  $F_{rev} = 0.131$  mm/rev in the Ti-64-Beta C workpiece (two alloy sample).

Figures 4–7 are presented in the same layout as Figure 3. Figure 4 shows the data for the Ti-64, Ti-CP and Beta C dissimilar FAST-DB billet. On the photograph three different surfaces can be seen which correspond to each of the three alloys. The depth map shows there is significant adhered material in both the Ti-CP and Beta C sections of the hole and that the surface finish is generally better in the Ti-64 region. The torque and  $F_z$  forces

increase sequentially as each alloy is drilled and the bond location is clearly identifiable from the force data. In this billet, there is significantly higher forces in the X axis of the dynamometer than the Y axis, especially during the start of the hole and while drilling Beta C. In the micrographs, the poor surface finish observed in the photograph and depth map can be seen at the machined surface within the Ti-CP. Some adhered material is also shown in the micrograph of the Ti-64 to Beta C bond. For both bonds there is minimal damage at the bond locations.

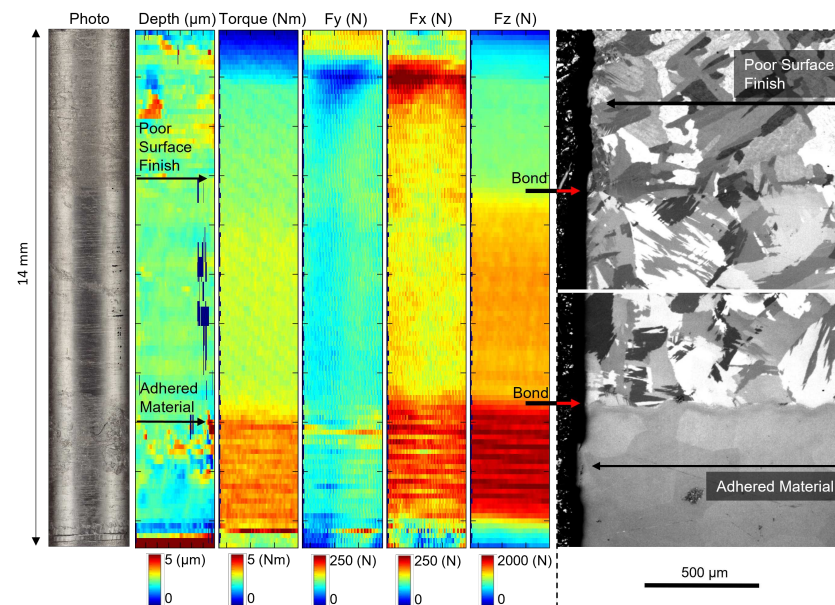


**Figure 4.** A photograph of the drilled surface, micrographs of the bond interfaces and depth, torque,  $F_y$ ,  $F_x$  and  $F_z$  maps for holes drilled at 1845 RPM and  $F_{rev} = 0.131$  mm/rev in the Ti-CP-Ti-64-Beta C workpiece (three alloy sample).

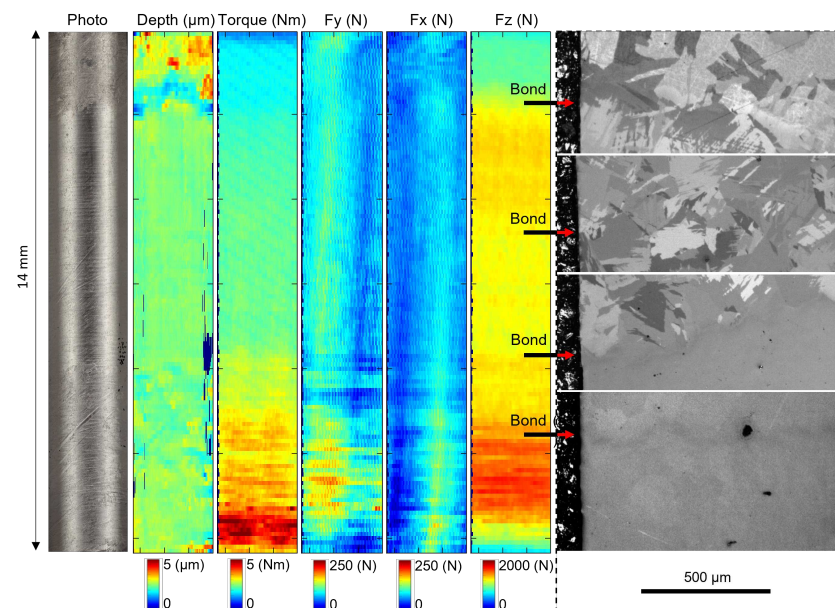


**Figure 5.** A photograph of the drilled surface, micrographs of the bond interfaces and depth, torque,  $F_y$ ,  $F_x$  and  $F_z$  maps for holes drilled at 1845 RPM and  $F_{rev} = 0.131$  mm/rev in the Ti-CP-Ti-6242-Ti-64-Ti-5553-Beta C workpiece (five alloy sample).

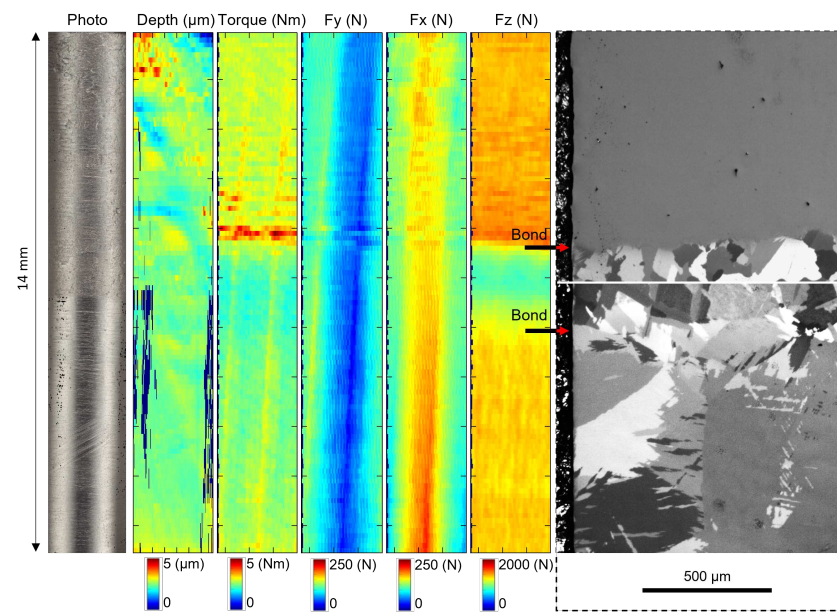


**Figure 6.** A photograph of the drilled surface, micrographs of the bond interfaces and depth, torque,  $F_y$ ,  $F_x$  and  $F_z$  maps for holes drilled at 1845 RPM and  $F_{rev} = 0.131$  mm/rev in the Beta C-Ti-CP-Ti-64 workpiece (three blind sample).

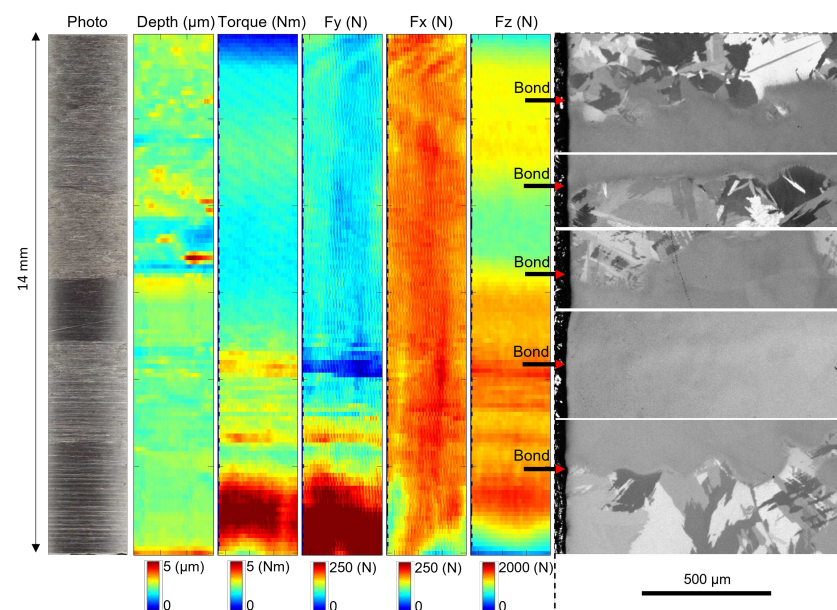


**Figure 7.** A photograph of the drilled surface, micrographs of the bond interfaces and depth, torque,  $F_y$ ,  $F_x$  and  $F_z$  maps for holes drilled at 1845 RPM and  $F_{rev} = 0.131$  mm/rev in the Ti-3-2.5-Ti-5553-Ti-CP-Ti-6242-Beta C-Ti-64 workpiece (n blind sample).

Figure 5 presents data for the open trial, five alloy billet (CP-Ti/Ti-6242/Ti-64/Ti-5553/Beta C). Within the photograph and depth map only four regions with different surface finishes can be discerned. The location of each alloy is shown on the micrographs and from the torque and force data. Again, the Ti-CP machined surface has a relatively bad surface finish with substantial amounts of adhered material. Ti-6242 and Ti-64 on the other hand, had the most consistent surface of the five alloys. For Ti-5553 and Beta C, small amounts of adhered material were observed on the machined surface. In the bond between Ti-CP and Ti-6242 there is surface depression before the bond where the machined surface has deformed, this is shown in both the micrograph and the depth map. In the Ti-64 and Ti-6242 bond there was no noticeable damage. Whereas, between Ti-64

and Ti-5553 there were minor variations of the machined surface depth, before and after the bond. Although the surface finish of the Ti-5553 and Beta C is not ideal, there was no noticeable damage in the bond between these two alloys. During the drilling of Beta C, and to a lesser extent Ti-5553, there were higher thrust forces and torque levels on the drill with considerably more variation in torque,  $F_x$ ,  $F_y$  and  $F_z$  than for the other alloys.

In Figure 6 the data for the first “blind” FAST-DB billet produced from three different alloys is presented. The photograph suggests there are two different surface finishes—suggesting that only two alloys exist in the blind billet at first glance. The depth map shows a poorer surface finish in the first alloy and there are no particular features at the bond. However, the  $F_z$  and torque data makes it easy to identify three alloys and the location of the two bonds. From this data alone, it was possible to identify the first alloy as Beta C, since it is the only alloy where  $F_z$  has reached 1800 N in previous billet samples. The second alloy was identified as Ti-CP, as it was the only alloy to have a  $F_z$  lower than 1000 N. The third alloy was the most difficult to identify but the pattern or fingerprint characterised in previous samples from the  $F_z$  data, identifies it as Ti-64. The  $F_z$  and  $F_x$  data did not change with depth of the drilled hole although the forces changed as the drill rotated through 360 degrees. There was no damage in either bond, as shown by the micrographs in Figure 6. In the micrographs, the Beta C surface was the worst of the three, this is also evident from the depth map. The surface finish of the Ti-64 and Ti-CP was generally good.

Figure 7 gives the data for the second blind billet for which the number of alloys bonded together was unknown to the investigators carrying out the force feedback analysis. From the photograph there were at least five recognisably different surface finishes which suggested at least five alloys. In the torque map, there were also five distinct regions, however, one of these regions did not correlate with the photograph, suggesting there was in fact six different alloys in the blind FAST-DB billet. The torque and  $F_y$  was relatively low in the first four alloys. In the fifth alloy, the torque and  $F_y$  was highly varied. In the final alloy the torque and  $F_y$  increased substantially as the drill exited the billet. The  $F_x$  for this sample was higher than in previous tests, suggesting the drill was poorly aligned in this axis. From the  $F_z$  data, it is possible to distinguish all the bonds apart from the bonds between the first two alloys. From the micrographs, there was minimal machining induced damage at the bonds except in the final bond where the damage was substantial.

#### 4. Discussion

The force feedback method established by Suarez et al. [20] for face-turning has proved invaluable during this drilling investigation. Its application for characterising where bonds exist within FAST-DB titanium billets has been demonstrated in Figures 3–7. In addition, the force feedback plots enabled researchers to correctly detect and state the stacking order of alloys in each of the two blind FAST-DB billets. By comparing the magnitude of the force and torque with the force feedback fingerprints for individual alloys, the authors were able to determine the three alloy (blind) sample in Figure 6. For the blind FAST-DB billet shown in Figure 7, the authors suggested that there were six alloys in the stacking sequence; Ti-64, Ti-5553, Ti-CP, Ti-6242, Beta C and Ti-64. The latter five alloys were correct, however, the first alloy was disclosed to be Ti-3-2.5, an alloy which had not yet been characterised in any previous tests. This demonstrates that the methodology can be used to recognise alloys, if those alloys have been drilled previously, and a reference force response exists for comparison. But when an alloy such as Ti-3-2.5 (which is a leaner version of Ti-64) is drilled, it is hard to distinguish that it is a new alloy and not one drilled previously.

Within the literature it has been established that titanium alloys with higher  $\beta$  phase content have poorer machinability, often this is characterised by higher forces and/or increased adherence of workpiece material to the machined surface or tool cutting edge [10,11]. This holds true when drilling FAST-DB dissimilar titanium alloy billets. However the direction in which alloys are drilled dictates the machinability characteristics of the process also. Directionality and the order in which alloys were drilled was shown to effect; (1) the

surface quality, (2) degree of the damage at the bonds and (3) the magnitude of force and torque measured for each alloy. For example, in the n blind sample (Figure 7), the forces associated with drilling Ti-5553 were lower than drilling Ti-6242, Beta C and Ti-64, as it was drilled at the start of the machining operation. Whereas, when Ti-5553 is drilled towards the bottom of the hole, as in the five alloy sample (Figure 5), the force is higher than any of the other alloys drilled in that hole. In a similar way, force and torque when drilling Ti-64 in the open trials, i.e., two and three FAST-DB alloy billets (Figures 3 and 4) are lower than Beta C, but in the n blind sample (Figure 7) the force and torque levels are higher. These excessive forces and the high variation in the force at the end of the hole indicates that stability becomes an issue when drilling multi-material workpieces. This is possibly due to chip jamming and/or poor hole cylindricity resultant from different titanium alloys having different diameters along the holes length.

Hardness is often used to categorise the machinability of materials [21]. In this work, the hardness measured for each alloy (shown in Figure 2) was significantly different. In addition, the hardness at the bonds was unpredictable. When an  $\alpha + \beta$  alloys is bonded to a more heavily stabilised  $\beta$  alloy, such as Ti-5553 or Beta C, the hardness at the bond was higher than in the bulk alloy regions. This is caused by diffusion of  $\beta$  stabilisers across the bond during the FAST-DB process. In turn this causes the formation of a local alloy chemistry that promotes the transformation of a fine scale secondary  $\alpha$  upon slow cooling—this results in high hardness [22]. Bonds where such a peak in hardness is observed, exhibit much higher cutting forces as the drill passes through the multi-material samples. Bonds that generate higher forces could drastically reduce the life of drill tools and cause excessive wear as an instant loading and unloading of the drill is analogous to low cycle fatigue. If bonds could be characterised based on their hardness values, it may be possible to program the machining process to accommodate for such features when machining multi-material workpieces.

In drilling, machining induced damage does not appear to manifest specifically at bond locations, as seen in the electron micrographs in Figures 4–7. There is some evidence that damage can occur around the bond in the form of either adhered material (or pick-up) Figure 4 and surface deformation. Figure 7, this damage appears more significant when the bond pairing contains two alloys which are highly dissimilar, such as when drilling from an  $\alpha + \beta$  to a  $\beta$  type alloy, such as in the bottom right micrograph in Figure 4. Unlike in turning, when drilling multi-materials in one stack, the stability of the operation (measured by the force consistency and magnitude) and the resulting hole quality and is reduced significantly as the number of alloys is increased. It seems, the more materials that are stacked within the billet, the more unstable the operation is and lower quality the hole surface will be. A similar result has been shown in the drilling of Ti/CFRP sacks [12]. Comparing the Alicona surface topography maps presented in Figures 4–7 against those which have been investigated in turning studies (CITE), it is clear there are some alloys, like Ti-CP and Beta C have similar tendency's to result in adhered chip material sticking to the machined surface. This is definitely concerning for the holes integrity as deposition of such material has been found to significantly decrease fatigue life as it causes fracture sites to be welded onto the surface [23]. Although this type of damage maybe exacerbated by the poor drill stability caused by multi-material drilling it has been found to be of concern when only one alloy is being drilled and so should not be considered solely a consequence of multi alloy drilling [24]. In general the findings of this study indicate that it is possible to drill multi alloy workpieces in a way which will mitigate severe reductions in machinability in terms of induced damage and hole quality.

## 5. Conclusions

- It is possible to drill multi-material workpieces without substantial surface or subsurface damage or hole quality issues at bond locations.
- When many alloys are drilled in a single workpiece the operation has poorer stability which can reduce hole quality.

- As in turning there is a directionality effect between each alloy pair, however for drilling there is also a more significant effect influenced by the number of alloys drilled in a workpiece and therefore stability.
- Smart drilling strategies can be implemented from the results presented in this work. It is better to machine  $\beta$  alloys at the very end of the machining operation and the machining of CP should be placed as closer to the contact point to avoid chemical contamination and that similar chemistry alloy compositions are easier to machine.
- Force feedback fingerprinting is effective for investigating aspects of multi-alloy machinability and can be used to identify the location of bonds within multi alloys.

By investigating the drilling machinability of multi alloy diffusion bonded materials this study has contributed to the groundwork that is required for adoption of diffusion bonded materials for commercial application. Further refinement the force feedback technique can be used to measure and quantify aspects of hole quality like cylindricity, providing the means for a relatively quick in process damage assessment tool that can be used widely within industry to monitor the health of parts.

**Author Contributions:** Conceptualization, A.G., O.L.B., D.S.F. and M.J.; methodology, A.G.; software, A.G. and D.S.F.; validation, A.G. and O.L.B.; formal analysis, A.G., O.L.B. and D.S.F.; investigation, A.G.; resources, M.J.; data curation, A.G. and D.S.F.; writing—original draft preparation, A.G.; writing—review and editing, A.G., O.L.B., D.S.F. and M.J.; visualization, A.G.; supervision, M.J.; project administration, M.J.; funding acquisition, M.J. All authors have read and agreed to the published version of the manuscript.

**Funding:** This research was funded by the EPSRC grant numbers EP/L016257/1 and EP/T024992/1.

**Data Availability Statement:** Not applicable.

**Acknowledgments:** We acknowledge Sandvik Coromant for support in providing resources for the experimental trials. Authors would like to thank Henry Royce Institute for Advanced Materials. Finally, the authors also thank Tom O’Sullivan for his contributions to the work and sample preparation.

**Conflicts of Interest:** The authors declare no conflict of interest.

## References

1. Metallurgy, P. *Titanium: Physical Metallurgy, Processing, and Applications*; Froes, F.H., ASM international: Novelty, OH, USA, 2015.
2. Joshi, V.A. *Titanium Alloys*; CRC Press: Boca Raton, FL, USA, 2006. [\[CrossRef\]](#)
3. Fernández, D.S.; Wynne, B.; Crawforth, P.; Fox, K.; Jackson, M. The effect of forging texture and machining parameters on the fatigue performance of titanium alloy disc components. *Int. J. Fatigue* **2021**, *142*, 105949. [\[CrossRef\]](#)
4. Lütjering, G. Influence of processing on microstructure and mechanical properties of ( $\alpha + \beta$ ) titanium alloys. *Mater. Sci. Eng. A* **1998**, *243*, 32–45. [\[CrossRef\]](#)
5. Cotton, J.D.; Briggs, R.D.; Boyer, R.R.; Tamirisakandala, S.; Russo, P.; Shchetnikov, N.; Fanning, J.C. State of the Art in Beta Titanium Alloys for Airframe Applications. *Jom* **2015**, *67*, 1281–1303. [\[CrossRef\]](#)
6. Levano Blanch, O.; Lunt, D.; Baxter, G.J.; Jackson, M. Deformation Behaviour of a FAST Diffusion Bond Processed from Dissimilar Titanium Alloy Powders. *Metall. Mater. Trans. A* **2021**, *52*, 3064–3082. [\[CrossRef\]](#)
7. Suarez, M.; Fernandez, A.; Menendez, J.; Torrecillas, R.; Kessel, J.H.U.; Kirchner, R.; Kessel, T. Challenges and Opportunities for Spark Plasma Sintering: A Key Technology for a New Generation of Materials. In *Sintering Applications*; IntechOpen: London, UK, 2013. [\[CrossRef\]](#)
8. Brinksmeier, E. Prediction of Tool Fracture in Drilling. *CIRP Ann.-Manuf. Technol.* **1990**, *39*, 97–100. [\[CrossRef\]](#)
9. Patil, S.; Kekade, S.; Phapale, K.; Jadhav, S.; Powar, A.; Supare, A.; Singh, R. Effect of  $\alpha$  and  $\beta$  Phase Volume Fraction on Machining Characteristics of Titanium Alloy Ti6Al4V. *Procedia Manuf.* **2016**, *6*, 63–70. [\[CrossRef\]](#)
10. Arrazola, P.J.; Garay, A.; Iriarte, L.M.; Armendia, M.; Marya, S.; Le Maître, F. Machinability of titanium alloys (Ti6Al4V and Ti555.3). *J. Mater. Process. Technol.* **2009**, *209*, 2223–2230. [\[CrossRef\]](#)
11. Graves, A.; Norgren, S.; Crawforth, P.; Jackson, M. A novel method for investigating drilling machinability of titanium alloys using velocity force maps. *Adv. Ind. Manuf. Eng.* **2021**, *2*, 100043. [\[CrossRef\]](#)
12. Xu, J.; El Mansori, M. Experimental study on drilling mechanisms and strategies of hybrid CFRP/Ti stacks. *Compos. Struct.* **2016**, *157*, 461–482. [\[CrossRef\]](#)
13. Uthayakumar, M.; Prabhakaran, G.; Aravindan, S.; Sivaprasad, J. Study on aluminum alloy piston reinforced with cast iron insert. *Int. J. Mater. Sci.* **2008**, *3*, 1–10.

14. Uthayakumar, M.; Prabhakaran, G.; Aravindan, S.; Sivaprasad, J. Influence of cutting force on bimetallic piston machining by a cubic boron nitride (CBN) tool. *Mater. Manuf. Process.* **2012**, *27*, 1078–1083. [[CrossRef](#)]
15. Saligheh, A.; Hajjalimohammadi, A.; Abedini, V. Cutting Forces and Tool Wear Investigation for Face Milling of Bimetallic Composite Parts Made of Aluminum and Cast Iron Alloys. *Int. J. Eng.* **2020**, *33*, 1142–1148.
16. Manikandan, G.; Uthayakumar, M.; Aravindan, S. Machining and simulation studies of bimetallic pistons. *Int. J. Adv. Manuf. Technol.* **2013**, *66*, 711–720. [[CrossRef](#)]
17. Levano Blanch, O.; Suárez Fernández, D.; Graves, A.; Jackson, M. MulTi-FAST: A Machinability Assessment of Functionally Graded Titanium Billets Produced from Multiple Alloy Powders. *Materials* **2022**, *15*, 3237. [[CrossRef](#)] [[PubMed](#)]
18. Suárez Fernández, D.; Jackson, M.; Crawforth, P.; Fox, K.; Wynne, B. Using machining force feedback to quantify grain size in beta titanium. *Materialia* **2020**, *13*, 100856. [[CrossRef](#)]
19. Naisson, P.; Rech, J.; Paris, H. Analytical modeling of thrust force and torque in drilling. *Proc. Inst. Mech. Eng. Part B J. Eng. Manuf.* **2013**, *227*, 1430–1441. [[CrossRef](#)]
20. Suárez Fernández, D.; Wynne, B.; Crawforth, P.; Jackson, M. Titanium alloy microstructure fingerprint plots from in-process machining. *Mater. Sci. Eng. A* **2021**, *811*, 141074. [[CrossRef](#)]
21. Mills, B. *Machinability of Engineering Materials*; Springer Science & Business Media: Berlin/Heidelberg, Germany, 2012.
22. Pope, J.J.; Calvert, E.L.; Weston, N.S.; Jackson, M. FAST-DB: A novel solid-state approach for diffusion bonding dissimilar titanium alloy powders for next generation critical components. *J. Mater. Process. Technol.* **2019**, *269*, 200–207. [[CrossRef](#)]
23. Cox, A.; Herbert, S.; Villain-Chastre, J.P.; Turner, S.; Jackson, M. The effect of machining and induced surface deformation on the fatigue performance of a high strength metastable  $\beta$  titanium alloy. *Int. J. Fatigue* **2019**, *124*, 26–33. [[CrossRef](#)]
24. Graves, A.; Norgren, S.; Crawforth, P.; Jackson, M. Surface roughness response to drilling of Ti-5Al-5Mo-5V-3Cr using Ti-Al-N PVD coated and uncoated WC/Co tools. *Procedia CIRP* **2020**, *87*, 170–175. [[CrossRef](#)]